

A quantitative measurement of spatial order in ventricular fibrillation

P.V. Bayly E.E. Johnson P.D. Wolf
H.S. Greenside W.M. Smith
R.E. Ideker

*From the Engineering Research Center
for Emerging Cardiovascular Technology
School of Engineering
Duke University*

*Durham, North Carolina 27708
and the Departments of Pathology and Medicine
Duke University Medical Center
Durham, North Carolina 27710*

*Supported in part by the National Institutes of Health
research grants HL-28429, HL-44066, and HL-33637
and the National Science Foundation
Engineering Research Center Grant CDR-8622201*

October 31, 2018

Abstract

Introduction: The degree of organization in ventricular fibrillation (VF) is not known. As an objective measurement of spatial order, spatial correlation functions and their characteristic lengths were estimated from epicardial electrograms of pigs in VF.

Methods: VF was induced by premature stimulation in 5 pigs. Electrograms were simultaneously recorded with a 22×23 array of unipolar electrodes spaced 1.12 mm apart. Data were obtained by sampling the signals at 2000 Hz for 20 minutes immediately after the initiation of VF. Correlations between all pairs of signals were computed at various times. Correlation lengths were estimated from the decay of average correlation as a function of electrode separation.

Results: The correlation length of the VF in pigs was found to be approximately 4-10 mm, varying as fibrillation progressed. The degree of correlation decreased in the first 4 seconds after fibrillation then increased over the next minute.

Conclusions: The correlation length is much smaller than the scale of the heart, suggesting that many independent regions of activity exist on the epicardium at any one time. On the other hand, the correlation length is 4 to 10 times the interelectrode spacing, indicating that some coherence is present. These results imply that the heart behaves during VF as a high-dimensional, but not random, system involving many spatial degrees of freedom, which may explain the lack of convergence of fractal dimension estimates reported in the literature. Changes in the correlation length also suggest that VF reorganizes slightly in the first minute after an initial breakdown in structure.

Key words: spatial correlation, correlation length, organization, dynamics, ventricular fibrillation, sudden death.

1 Introduction

The ventricular myocardium is a nonlinear, excitable system which can appear almost totally synchronized in sinus rhythm, or completely disorganized in fibrillation. Fifty years ago Wiggers described four stages of ventricular fibrillation; his classification relies strongly on qualitative descriptions of the degree of spatial organization such as “undulatory contractions” (stage 1), “convulsive incoordination” (stage 2), “tremulous incoordination” (stage 3), and “feeble contraction wavelets” (stage 4) [1]. Reentrant spatial structures such as wavelets or rotors are thought to provide the underlying mechanism of VF. Rotating activation patterns have been observed in experiments in animals and in isolated myocardium [2, 3, 4, 5]; they have also been widely studied in mathematical models of excitable media [6, 7, 8]. In general, greater spatial order is associated with fewer, larger structures. In this paper we explore an objective measure of the *amount* of spatial organization: the spatial correlation length.

Many investigators have examined the organization of activation in the heart by detecting potentials at a number of locations in the myocardium with an array of spatially distributed electrodes [3, 9, 10]. Organization and spatial structure have been documented by following the progress of individual waves of activation. Isochronal maps, which depict the position of the wave front as time progresses, or isopotential maps, which show lines of constant voltage on the surface of the heart at a single instant, illustrate the size and type of waveforms which occur during VF. Isochronal maps are more commonly used than isopotential plots, since one map can show the position of the wave front at many instants of time. However, objective, statistical descriptions of activity are also needed to compare with results from simulations and from other experiments.

The question of spatial organization is related to the widely speculated relationship between nonlinear dynamics, chaos, and fibrillation [11, 12, 13]. The mathematical term “chaos” refers specifically to the temporally aperiodic, unpredictable behavior of some nonlinear deterministic systems characterized by broad-band power spectra and extreme sensitivity to initial conditions. A necessary condition for chaos is at least one positive Lyapunov exponent, which describes the exponential separation of nearby orbits. The concepts of strange attractors and chaos have illuminated the behavior of simple, few degree-of-freedom, nonlinear systems. The methods of low-dimensional

chaos also apply to the nonlinear dynamics of multi-degree-of-freedom systems which involve very few modes [14] such as an oscillating fluid system [15].

Temporally complicated, but spatially organized, behavior of extended systems may often be well modeled by low-dimensional chaos. In these cases one may obtain useful quantities, like Lyapunov exponents, and analyze simplified models which retain the basic mechanisms of instability and disorder. Spatially incoherent dynamics in an extended system are inherently high-dimensional, meaning that many independent variables are required to describe its state. These cases are impractical to treat as chaotic [16]. Because of this difference, determining the degree of spatial organization of VF is important in developing useful models of fibrillation and finding effective clinical countermeasures.

In other fields, notably fluid mechanics, a numerical measure of the characteristic size of a spatial process has frequently been extracted: the correlation length. There is more than one definition of the correlation length; the quantity, λ , used here describes the rate of decay of the spatial correlation function as a function of distance. It has been calculated for many experiments, and has been interpreted as the characteristic length scale of the typical spatial structure in the experiment: the diameter of the average wavelet, eddy, or rotor, for example [17, 18, 19, 20, 21].

While VF has been the subject of much study and more speculation, an objective, quantitative description of its spatial organization has not been put forward. Clear experimental results are needed to compare with the burgeoning supply of data from numerical models [22, 23]. In this study, the correlation length of ventricular fibrillation has been calculated for several intervals, at various times after the initiation of VF, in each of five pig hearts. The application of the method and the experimental procedure are explained in more detail below.

2 Methods

2.1 Spatial correlation function

The spatial correlation function, $R(dx)$, is a scalar function describing the average correlation between all pairs of measurements separated by the vector

$d\mathbf{x}$. For a general, real-valued function of time and space, $g(t, \mathbf{x})$, the spatial correlation function is [24]:

$$R(d\mathbf{x}) = E\{g(t, \mathbf{x})g(t, \mathbf{x} + d\mathbf{x})\}, \quad (1)$$

where E denotes an ensemble average. For a stationary, ergodic process, the value of the spatial correlation function is obtained from the following integral. Integration is over the time interval $-T$ to T and over the spatial domain S .

$$R(d\mathbf{x}) = \lim_{T \rightarrow \infty} \frac{1}{2T} \int_S \int_{-T}^T g(t, \mathbf{x})g(t, \mathbf{x} + d\mathbf{x}) dt d\mathbf{x}. \quad (2)$$

The spatial correlation function is completely analogous to the commonly encountered temporal autocorrelation function,

$$A(\tau) = \lim_{T \rightarrow \infty} \frac{1}{2T} \int_{-T}^T f(t)f(t + \tau) dt. \quad (3)$$

Sampling the continuous process, $g(t, \mathbf{x})$, with a 2-dimensional array of equally spaced sensors leads to a set of discrete measurements. If P time samples are taken from each sensor of an $M \times N$ array, one obtains the values:

$$c_{ijk} = g(t_k, \mathbf{x}_{ij}), \quad i = 1, 2, \dots, M, \quad j = 1, 2, \dots, N, \quad k = 1, 2, \dots, P, \quad (4)$$

where t_k is the time of the k^{th} sample and \mathbf{x}_{ij} is the location of the sensor in the i^{th} row and j^{th} column of the sensor array. For a regularly spaced array with a separation of h units between adjacent sensors, $\mathbf{x}_{ij} = [h(i - 1), h(j - 1)]^T$, and $d\mathbf{x} = [h \Delta i, h \Delta j]^T$.

The spatial correlation function of this discrete data set is ideally approximated by the sum:

$$R(\Delta i, \Delta j) = \frac{1}{Q(\Delta i, \Delta j)} \sum_{i=1}^M \sum_{j=1}^N \sum_{k=1}^P c_{ijk}c_{(i+\Delta i)(j+\Delta j)k}. \quad (5)$$

Here $Q(\Delta i, \Delta j)$ is the total number of simultaneous samples which are separated in space by the the vector $[\Delta i, \Delta j]^T$. The quantities Δi and Δj may vary from $-(M - 1)$ to $(M - 1)$ and from $-(N - 1)$ to $(N - 1)$, respectively.

The resulting estimates of spatial correlation are only statistically valid for values of Δi and Δj which allow an adequate number of correlations

to be averaged; for example, in an $M \times N$ array there are only two sensors separated by a displacement of $[(M-1), (N-1)]^T$, but MN sensors separated by the displacement $[0, 0]^T$. Accordingly, correlations will not be presented for separations larger than $3/4$ of the shorter side of the rectangular array.

Just as the temporal autocorrelation function of a harmonic signal is a sinusoidal curve with the same period, the spatial correlation function of a travelling plane wave is a sinusoidal surface with the same wavelength (Figure 1). The spatial correlation function of uncorrelated random noise is close to zero everywhere except at the origin (Figure 2). In many real, physical systems (turbulent fluids, capillary waves), the envelope of the correlation function does not remain constant, as in the perfectly ordered plane wave, nor does it vanish as in the case of the random noise. Instead, it usually decays at some characteristic rate. For small $|\mathbf{dx}|$ the decay can be assumed to be exponential, as:

$$R(|\mathbf{dx}|) \propto e^{-|\mathbf{dx}|/\lambda}. \quad (6)$$

To illustrate how we extract the correlation length, Figure 3a shows a typical decaying correlation, R , plotted as a function of the vector separation between sensors, $[dx, dy]^T$. The solid curve of Figure 3b is obtained by averaging the surface of Figure 3a over all angles to obtain a plot of R vs $|\mathbf{dx}|$. The decay of the correlation curve is described by the parameter, λ , obtained from a least-squares exponential curve fit also shown in the Figure 3b. Two numbers can be extracted from the original curve of correlation vs separation: L_e is the length needed for the correlation to decay to $1/e$, and L_0 is the value of $|\mathbf{dx}|$ at which the correlation first drops to zero. L_e may be used as a check on the value of λ .

Although the exponential curve is not always the optimal fit, it is a simple, straightforward, repeatable, and widely used approach. Values of λ vary quite closely with values of L_e (see Figure 3 and Table 1). It is impractical to use L_e or L_0 if not all curves decay to $1/e$ or 0.

A wide variety of processes have been characterized by their correlation lengths. Hohenberg and Shraiman in reference [20] used the correlation length, λ , to describe the degree of coherence of one of the simplest numerical models of disorder in a spatially extended nonlinear system: the 1-dimensional Kuramoto-Sivashinsky equation. Tuffiaro and colleagues in [19] studied the correlation length of a system of small surface waves in water as a forcing parameter was varied. Coulet and coworkers in [21], recently

used λ as a quantitative measure of spatial organization in numerical studies of the complex Ginzburg-Landau equation, a 2-D system which exhibits spiral patterns. They show that for their model, the spatial correlation length corresponds specifically to the mean distance between spiral “defects”, which is presumably also the average diameter of the structures [21]. Although no systematic evidence is presented of such a specific meaning for the correlation length of fibrillation, we interpret it as roughly the average length of a patch of coherent activity.

2.2 Experiment

Fibrillation data were obtained from 5 anesthetized pigs, each weighing approximately 25-27 kg. The animals were anesthetized with pentothal 5%, and respiration was supported by a mechanical ventilator. Anesthesia and fluid levels were maintained with an intravenous line. A line from the femoral artery allowed the continuous monitoring of hemodynamic status and blood gas values. The animals received doses of the drugs ketamine and acepromazine before anesthesia was started, and intravenous succinylcholine was used to induce and maintain skeletal muscle paralysis. Normal blood gas, electrolyte, and body temperature levels were maintained.

The chest was opened using a median sternotomy, and the heart was exposed and suspended in a pericardial cradle. The electrode plaque was sutured to the epicardium of the right or left ventricle. The electrode plaque is a plastic block containing 524 Ag-AgCl electrodes, 506 of which form a 22×23 array. The electrodes in the grid are spaced 1.12 mm apart, providing total dimensions of 2.35×2.46 cm. A photograph of the array is provided in Figure 4. The electrode spacing was chosen to avoid significant spatial aliasing while allowing the plaque to cover as large an area as possible. A previous study has provided evidence that very little spatial aliasing error is introduced with 1.12 mm spacing [25].

VF was induced by applying a premature stimulus to the ventricular muscle. In this procedure the muscle was paced with relatively small, regular, current stimuli (S1 stimuli) applied to the myocardium through a stainless steel electrode. The stimulus electrode was sutured to the epicardium about 1 cm from the electrode array. The S1 stimuli were spaced 350 ms apart and each pulse delivered current equal to twice the diastolic threshold. After 10 equally spaced S1 pulses were applied, a larger (50 mA) current stimulus, S2,

was applied through another stainless steel electrode located 1 to 2 cm away. The S2 stimulus was applied prematurely, while some of the tissue was still in an inexcitable state from the previous S1 beat. The large, premature stimulus is believed to induce rotors as it intersects the partially refractory region [2]. This method is somewhat analogous to the procedure used by Davidenko and colleagues to initiate rotating waves in isolated sheep myocardium [5], and to the initial conditions used by Barkley and others in numerical models of other excitable media [6]. Reference [26] describes the experiment in more technical detail.

Simultaneous time series of the electrical potential at each of the electrodes were recorded with 14-bit precision at a sampling rate of 2000 Hz, using a 528-channel mapping system [27]. The signals were prefiltered with a 500 Hz low-pass filter to prevent temporal aliasing and with a 0.5 Hz high-pass filter to eliminate low-frequency artifact. These frequency cutoffs are well removed from the characteristic frequency of VF in pigs, which is usually near 10 Hz [28]. Potentials were measured relative to a reference voltage from the animal's left leg.

For each experiment, 20 minutes of data were recorded immediately after VF was induced. Subsets of these data were taken from the first few seconds of fibrillation, and after 15 seconds, 30 seconds, 1 minute, 2 minutes, 5 minutes, and 10 minutes of VF. Several spatial correlation functions were calculated using one-second blocks of data taken from each time interval. The one-second block size was chosen to ensure stationarity in time while including several cycles of activation; in several test cases the time interval was varied from 0.1 to 1.0 seconds, with only slight quantitative effects.

3 Results

A typical time series recorded at a single electrode just after the initiation of fibrillation is shown in Figure 5. Figure 6 displays a sequence of spatial patterns recorded by the electrode grid in the first second after the initiation of VF. The spatial oscillations do not appear to be smaller than the size of the array. Two seconds later the structure seems to have broken up, as the sequence in Figure 7 indicates. By 60 seconds, however, larger structures have reappeared (Figure 8).

Spatial correlation estimates track these changes in organization con-

sistently. Figure 9 shows the spatial correlation computed from one-second blocks of data in the first, second, third and sixty-first seconds after the initiation of VF in one heart (experiment #3). In the first second the correlation surface falls off relatively slowly from the peak at the origin (Figure 9a). As disorganization increases (more structures of smaller size) the fall-off becomes more rapid (Figures 9b, 9c) and the surfaces approach the delta function of Figure 2. However, at 60 seconds the fall-off is noticeably less sharp (Figure 9d).

To extract a correlation length from the surface of spatial correlation the correlation estimate was averaged over all directions. Curves of average correlation vs. magnitude of separation are shown in Figure 10; these curves were obtained by averaging the spatial correlation surfaces of Figure 9.

The curves in Figure 10 decay roughly exponentially, and were fitted using a least squares algorithm. The constant, λ , for each curve is tabulated in Table 1. The length needed for the correlation to decay to a value of $1/e$, L_e , and the value of the first zero-crossing of the curve, L_0 , are also presented. It is apparent that λ , L_e and L_0 vary together. We can also see that the qualitatively more organized behavior has a longer correlation length.

Time	λ	L_e	L_0
1 sec	11.4	10.2	> 15.0
2 sec	6.3	6.0	10.8
3 sec	5.0	4.6	9.5
60 sec	8.7	7.9	12.7

Table 1: Characteristic lengths (in mm) obtained from the correlation curves of Figure 9 (experiment #3): the correlation length or constant of exponential spatial decay, λ ; the length to decay to $1/e$, L_e ; and the first zero-crossing, L_0 .

Figures 11 and 12 show spatial correlation vs. vector separation and spatial correlation vs. the magnitude of separation for an episode of fibrillation in a different heart (experiment #4). Although the progress of the arrhythmia is different, the characteristic correlation curves of Figure 12 are

qualitatively similar to those in Figure 10. The differences in the correlation length capture the quantitative differences in spatial organization.

Similar analyses were performed for each of the five experiments and correlation lengths were calculated for data at various times during VF. Table 2 provides a summary of the correlation lengths calculated at several different times, for each experiment. The correlation lengths fall mostly between 4 mm and 10 mm.

Time	Exp #1	Exp #2	Exp #3	Exp #4	Exp #5
1 sec	11.3	5.9	11.4	6.1	3.8
3 sec	4.4	3.3	5.0	5.2	3.7
15 sec	4.8	3.7	6.0	6.0	4.1
30 sec	4.8	4.8	7.6	4.7	3.7
60 sec	5.0	5.4	8.7	8.1	5.0
120 sec	6.0	5.3	6.7	8.4	4.6
300 sec	5.4	4.8	5.3	6.7	4.2
600 sec	5.7	4.9	5.7	6.4	4.1

Table 2: Correlation lengths, λ , (in mm) calculated from VF data during the progression of fibrillation in 5 experiments. Each value was calculated from a one-second block of data recorded at the indicated time after the initiation of VF.

In this study it was found that the correlation length of VF decreased over the first few seconds but often increased as fibrillation progressed; in each experiment the correlation length after 3 seconds was shorter than both the correlation length after 1 second and the correlation length after 60 seconds. These differences were statistically significant with $p < 0.05$. The mean correlation lengths (over the 5 experiments) as VF progressed are shown in Figure 13.

4 Discussion

4.1 Interpretation of results

The correlation length is a widely used measurement of spatial organization which can be used to estimate the degree of spatial organization of physical processes. Longer correlation lengths are associated with larger structures and apparently more organized behavior. This study suggests that correlation lengths may be extracted from experimental epicardial electrograms and that those lengths may be used to compare different stages and types of ventricular fibrillation.

Moe and his co-workers postulated in 1964 that the size and number of wavelets in the “wandering wavelet” model of ventricular fibrillation was critical to the development of an episode of fibrillation [29]. The broad interpretation of spatial correlation is not restricted to a certain physical process, nor does it explicitly provide evidence for a particular mechanism (such as wandering wavelets, or spiral waves). The physical mechanism should, however, be consistent with the specific numerical values of the correlation length.

The initial breakup of organization during fibrillation was first observed years ago. It is described by Wiggers as the transition between “undulatory” motion and “convulsive incoordination” [1]. The apparent reorganization of VF after 30-60 seconds is not well known, but is consistent with the greater low-frequency content of typical temporal power spectra observed as fibrillation progresses [28, 30]. Such restructuring may be due to a coalescence of small structures into larger ones as time passes, perhaps related to the changing parameters of the myocardium. Worley and colleagues noted decreased activation rates in epicardial electrograms during the first few minutes of VF in dogs; changes in activation rate on the endocardium were much smaller [31]. These effects were attributed to the ischemic condition of the heart. Numerical models have shown that even for fixed parameters, coalescence of disorganized behavior into structures such as stable rotors can occur [23].

Can observed correlation lengths illuminate any aspect of the relationship between low-dimensional chaos and fibrillation? The correlation length of VF in pigs was found to vary between 4 and 10 mm. Simple scaling arguments can be used to establish a rough measure of the global complexity of fibrillation. If the correlation length corresponds to the length of the average coherent structure on the epicardium, each such region would have an area

of 16-100 mm². The surface area of the ventricular epicardium in a typical pig heart may be about 7500 mm². The ratio of these two areas implies that at a given instant, there exist 75 to 500 approximately independent areas of activity on the epicardium. This rough estimate of the number of coherent regions, although probably an upper bound (see Section 4.2), provides evidence that VF is too complicated to be modeled as a low-dimensional, few-degree-of-freedom, system. Such evidence could explain the lack of convergence of the correlation dimension which has been reported by previous authors [12, 32]. Our results suggest that treating VF as low-dimensional chaos is unlikely to succeed in models or in clinical strategies.

On the other hand these results strongly support the claim, recently made in a study by Damle and co-workers [33], that VF in dogs is not random. Damle et al. showed that the directions of activation recorded by adjacent electrodes (separated by 2.5 mm) were related. This is consistent with our observations because the adjacent electrodes were closer than a correlation length apart. Damle et al. also document the decline in the amount of spatial “linking” over the first 5 seconds of VF. They did not examine longer episodes of VF. The finite correlation lengths we observed also provide direct evidence that VF is not a spatially random process. Instead, both studies indicate that VF is a high-dimensional process, but with a measurable degree of coherence.

4.2 Limitations

The estimate of 75 to 500 independent regions calculated above might be interpreted as a generous *upper bound* on the number of activation fronts which exist simultaneously on the epicardium. The size of the electrode array, which covers perhaps 5-10% of the area of the ventricular epicardium, prevents the observation of high correlations between events further apart than the length of the array. Thus, for behavior with a characteristic wavelength larger than the size of the array, the estimate of correlation length is biased downwards. Also, our statistic measures correlations between simultaneous events, so two sites exhibiting similar activity at different times will appear under-correlated. Finally, the choice of the unscaled correlation length λ , rather than say 2λ , to represent the length of a “correlated” region represents a conservative and somewhat arbitrary decision.

Averaging over the area of the array and over one-second blocks of

time may diminish the contributions of local or short-lived organized processes. However, the spatial correlation function is independent of any temporal variability during the averaging time. For example, as long as their spatial properties are the same a stationary spiral wave will have the same correlation length as a drifting spiral, though their local temporal signals will be quite different. As another example, if an identical, temporally random, signal were recorded by each electrode, the electrodes would still be perfectly correlated.

No evidence has been presented of a direct relationship between the correlation length and any other specific quantity measured during VF. Some of the conclusions drawn in this paper are based on analogies to other distributed systems: notably fluid experiments and numerical simulations. Improved experiments and methods of analysis may allow the calculation of the mean distance between reentrant loops, or a similar quantity, to firmly establish the absolute meaning of the correlation length in fibrillation. A possible length scale for comparison is the width of the region of electromotive activity during fibrillation, which was recently reported by Witkowski and colleagues [34] to be between 0.5 and 1.0 mm in dogs; this quantity is roughly an order of magnitude smaller than our estimated correlation lengths.

Although our measurements were taken from a 2-dimensional array, VF occurs in a 3-dimensional medium. It has been shown that well-defined 3-D structures can produce apparently spatially complex patterns of activity on a 2-D surface [35]. Therefore it is quite possible that even though the 2-D patterns may be well characterized, the underlying 3-D process is not.

4.3 Implications

It is potentially extremely useful to measure quantities which are associated with organization. If the break-up or coalescence of reentrant waves is part of the mechanism of fibrillation or defibrillation, then a measure of the coherence of VF must be important to the clinician or the electrophysiologist. Drugs may be compared by studying whether, or how much, they increase or decrease spatial organization. Does more organization make it more or less difficult to defibrillate? Does the optimal defibrillation strategy depend to the spatial nature of the arrhythmia? Is a high degree of organization associated with a tendency to spontaneously defibrillate? Is the size of a rotor related to the size of the smallest heart that will sustain fibrillation?

It is possible to answer these questions only if it is possible to compare unbiased measures of spatial structure. The correlation length is a repeatable and objective measure of relative organization. The description of spatial organization in VF by such a quantity is a useful step toward understanding and effectively treating fibrillation.

Acknowledgements

We wish to acknowledge and thank Michael Yarger, Ed Simpson, and Sharon Melnick for their considerable help, and D. Kaplan for his helpful comments. Computational aspects of this work were supported by a grant of computer time from the North Carolina Supercomputer Center.

References

- [1] C.J. Wiggers. The mechanism and nature of ventricular defibrillation. *American Heart Journal*, pages 399–412, 1940.
- [2] D.W. Frazier, P.D. Wolf, J.M. Wharton, A.S.L. Tang, W.M. Smith, and R.E. Ideker. Stimulus-induced critical point: Mechanism for electrical initiation of reentry in normal canine myocardium. *J. Clinical Investigation*, pages 1039–1052, 1989.
- [3] M.A. Allesie, F.I.M. Bonke, and F.J.G. Schopman. Circus movement in rabbit atrial muscle as a mechanism of tachycardia. iii. the “leading circle” concept: A new model of circus movement in cardiac tissue without the involvement of an anatomical obstacle. *Circulation Research*, pages 9–18, 1977.
- [4] R.E. Ideker, D.W. Frazier, W. Krassowska, N. Shibata, P-S. Chen, K.M. Kavanagh, and W.M. Smith. Experimental evidence for autowaves in the heart. *Annals of the New York Academy of Sciences*, 519:208–218, 1990.
- [5] J.M. Davidenko, A.V. Pertsov, R. Salomonsz, W. Baxter, and J. Jalife. Stationary and drifting spiral waves of excitation in isolated cardiac muscle. *Nature*, pages 349–351, 1992.

- [6] Dwight Barkley. A model for fast computer simulation of waves in excitable media. *Physica D*, 49:61–70, 1991.
- [7] J.P. Keener. A geometrical theory for spiral waves in excitable media. *SIAM J. Appl. Math.*, pages 1039–1056, 1986.
- [8] M. Gerhardt, H. Schuster, and J.J. Tyson. A cellular automaton model of excitable media including curvature and dispersion. *Science*, pages 1563–1566, 1990.
- [9] R.E. Ideker, G.J. Klein, L. Harrison, W.M. Smith, J. Kasell, K. Reimer, A.G. Wallace, and J.J. Gallagher. The transition to ventricular fibrillation induced by reperfusion after acute ischemia in the dog: a period of organized epicardial activation. *Circulation*, 63(6):1371–1379, 1981.
- [10] N. El-Sherif, R. Mehar, W.B. Gough, and R.H. Zeiler. Ventricular activation patterns of spontaneous and induced ventricular rhythms in canine one-day-old myocardial infarction: Evidence for focal and reentrant mechanisms. *Circulation Research*, pages 152–166, 1982.
- [11] A.L. Goldberger, V. Bhargava, B.J. West, and A.J. Mandell. Some observations on the question: Is ventricular fibrillation ‘chaos’? *Physica D*, 19:282–289, 1986.
- [12] D. Kaplan and R. Cohen. Is fibrillation chaos? *Circulation Research*, 67:886–892, 1990.
- [13] M.R. Guevara and L. Glass. Phase locking, period-doubling bifurcations, and irregular dynamics in periodically stimulated cardiac cells. *Science*, pages 1350–1353, 1981.
- [14] P.J. Holmes. Nonlinear dynamics, chaos, and mechanics. *Applied Mechanics Review*, 43:S23–S29, 1990.
- [15] H.L. Swinney and J.P. Gollub. Characterization of hydrodynamic strange attractors. *Physica D*, 18:448–454, 1986.
- [16] J. Guckenheimer. Dimension estimates for attractors. *Contemporary Mathematics*, pages 357–367, 1984.

- [17] S. Panchev. *Random Functions and Turbulence*. Pergamon Press, New York, 1971.
- [18] J.L. Lumley. *Stochastic Tools In Turbulence*. Academic Press, New York, 1970.
- [19] N.B. Tufillaro, R. Ramashankar, and J.P. Gollub. Order-disorder transition in capillary waves. *Physical Review Letters*, 62:422–425, 1989.
- [20] P.C. Hohenberg and B.I. Shraiman. Chaotic behavior of an extended system. *Physica D*, pages 109–115, 1989.
- [21] P. Couillet, L. Gil, and J. Lega. Defect-mediated turbulence. *Physical Review Letters*, pages 1619–1622, 1989.
- [22] A.V. Panfilov and A.V. Holden. Spatiotemporal irregularity in a two-dimensional model of cardiac tissue. *Int'l. J. Bifurcation and Chaos*, pages 219–225, 1991.
- [23] M. Markus, M. Krafczyk, and B. Hess. Randomized automata for isotropic modelling of two- and three-dimensional waves and spatiotemporal chaos in excitable media. In A.V. Holden, M. Markus, and H.G. Othmer, editors, *Nonlinear Wave Process In Excitable Media*, pages 161–182. Plenum Press, New York, 1989.
- [24] W.K. Pratt. *Digital Image Processing*. John Wiley & Sons, New York, 1978.
- [25] P.V. Bayly, E.E. Johnson, S.F. Idriss, R.E. Ideker, and W.M. Smith. Minimum electrode spacing for mapping ventricular fibrillation using spatial sampling theory. In *Proc. Computers in Cardiology*, Oct. 1992.
- [26] E.E. Johnson, D.L. Rollins, P.D. Wolf, W.M. Smith, and R.E. Ideker. Mechanism of ventricular fibrillation as mapped with 524 closely spaced simultaneously recorded epicardial electrodes. *Circulation*, pages I–820, 1992.
- [27] P.D. Wolf, D.L. Rollins, T.F. Blitchington, R.E. Ideker, and W.M. Smith. Design for a 512 channel cardiac mapping system. In D.C.

- Mikulecky and A.M. Clarke, editors, *Biomedical Engineering: Opening New Doors. Proceedings of the Fall 1990 Annual Meeting of the Biomedical Engineering Society*, pages 5–13, New York, 1990. New York University Press.
- [28] E.E. Johnson, S.F. Idriss, C. Cabo, S.B. Melnick, W.M. Smith, and R.E. Ideker. Evidence that organization increases during the first minute of ventricular fibrillation in pigs mapped with closely spaced electrodes. *J. American College Cardiology*, page 90A, 1992.
- [29] G.K. Moe, W.C. Rheinbolt, and J.A. Abildskov. A computer model of atrial fibrillation. *American Heart Journal*, pages 200–220, 1964.
- [30] J.H. Herbschleb, R.M. Heethaar, I. van der Tweel, and F.L. Meijler. Frequency analysis of the ECG before and during ventricular fibrillation. In *Proc. Computers in Cardiology*, pages 365–368, 1980.
- [31] S.J. Worley, J.L. Swain, P.G. Colavita, W.M. Smith, and R.E. Ideker. Development of an endocardial-epicardial gradient of activation rate during electrically induced, sustained, fibrillation in dogs. *American J. Cardiology*, pages 813–820, 1984.
- [32] F. Ravelli and R. Antolini. Dimensional analysis of the ventricular fibrillation ECG. In A.V. Holden, M. Markus, and H.G. Othmer, editors, *Nonlinear Wave Processes in Excitable Media*, pages 335–342. Plenum Press, 1989.
- [33] R.S. Damle, N.M. Kanaan, N.S. Robinson, Y. Ge, J.J. Goldberger, and A.H. Kadish. Spatial and temporal linking of epicardial activation patterns during ventricular fibrillation in dogs: evidence for underlying spatial organization. *Circulation*, pages 1547–1558, 1992.
- [34] F. Witkowski, P.A. Penkoske, and K.M. Kavanagh. Estimate of electromotive surface dimension during ventricular fibrillation. In *Proc. IEEE Engineering in Medicine and Biology Society Conference*, pages 32–33, 1991.
- [35] A.T. Winfree. *The Geometry of Biological Time*, chapter 9. Springer-Verlag, New York, 1980.

Figures

Figure 1.

The spatial correlation function of artificial data which are periodic in time and 2-dimensional space: $f(x, y, t) = \sin(4t - 2x - y)$. a) The spatial pattern, $f(x, y, t_0)$, observed at one instant in time (a snapshot of the traveling wave). b) The correlation, R , as a function of displacement, or spatial lag, $[dx, dy]^T$. The data consisted of 100 time samples at each “sensor” of a 15×15 spatial array.

Figure 2.

Same as Figure 1. except that data which was generated by a UNIX random number generator: $f(x, y, t) = \text{random}()$. a) Random instantaneous spatial pattern. b) Correlation vs vector displacement: the spatial correlation is approximately a delta-function (zero everywhere except at the origin).

Figure 3.

a) A typical surface of correlation vs. separation vector (spatial lag). b) The corresponding curve of correlation vs. magnitude of sensor separation. Also shown are the characteristic constants λ , L_e , and L_0 . Data was from 1000 samples of VF at each sensor of a 22×23 array.

Figure 4.

Photograph of the electrode array. Silver/silver chloride electrodes are arranged in a 22×23 grid with 1.12 mm inter-electrode spacing.

Figure 5.

A representative time series of VF recorded at one electrode, one second after fibrillation was induced by a premature (S2) stimulus. The sampling frequency was 2000 samples/sec.

Figure 6.

Spatial patterns of electrode potentials recorded by the 22×23 array during the passage of an activation front 1 second after the beginning of VF. Darkest pixels represent potentials of less than -2 millivolts; lighter pixels represent progressively higher potentials up to +2 millivolts; potentials of +2 millivolts and higher correspond to the lightest grey level. (“Bad” electrodes are responsible for some isolated anomalous pixels). Panels represent “snapshots”

of the array at a) $t=1.230$ sec. b) $t=1.250$ sec. c) $t=1.270$ sec. d) $t=1.290$ sec.

Figure 7.

The spatial patterns of electrode potentials recorded by the array 3 seconds after the beginning of VF. a) $t=3.210$ sec. b) $t=3.230$ sec. c) $t=3.250$ sec. d) $t=3.270$ sec.

Figure 8.

Patterns of electrode potentials 1 minute after VF was induced. a) $t=61.690$ sec. b) $t=61.710$ sec. c) $t=61.730$ sec. d) $t=61.750$ sec.

Figure 9.

Surfaces of spatial correlation of fibrillation vs separation vector for experiment #3. Correlations were computed from 1.0 seconds of data at each sensor of a 22×23 electrode array. a) 1.0 seconds to 2.0 seconds after VF was induced. b) 2.0 - 3.0 seconds. c) 3.0 - 4.0 seconds. d) 60.0 - 61.0 seconds.

Figure 10.

Curves of spatial correlation vs magnitude of separation for experiment #3. The radial distance from the origin of Figures 8a-d) to each grid point is the magnitude of separation. See Table 2 for the correlation lengths corresponding to each curve.

Figure 11.

Surfaces of spatial correlation vs separation vector for experiment #4. a) 1.0 - 2.0 seconds. b) 2.0 - 3.0 seconds. c) 3.0 - 4.0 seconds. d) 60.0 - 61.0 seconds.

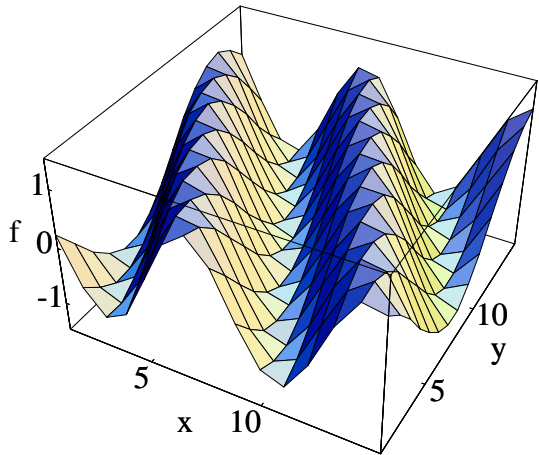
Figure 12.

Curves of spatial correlation vs magnitude of separation for experiment #4. See Table 2 for the corresponding correlation lengths.

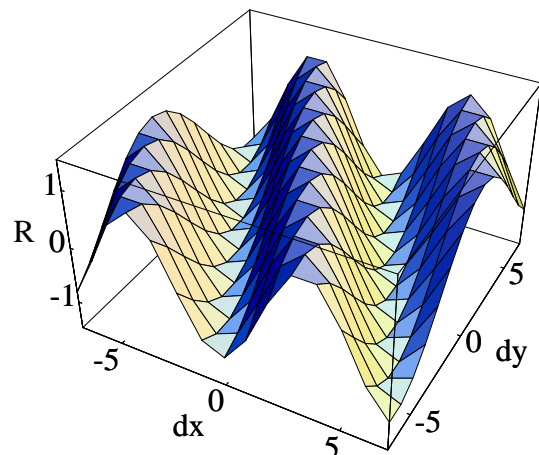
Figure 13.

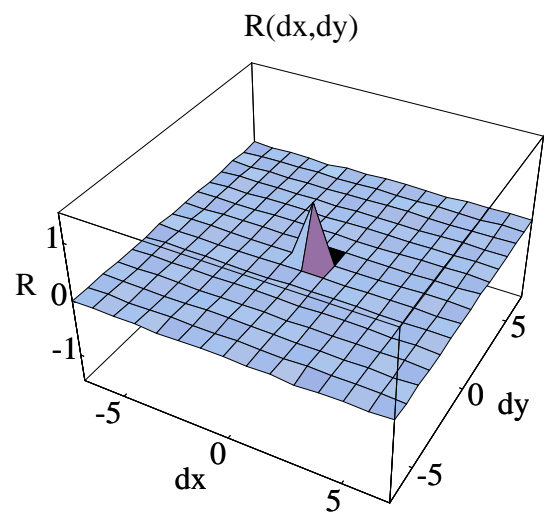
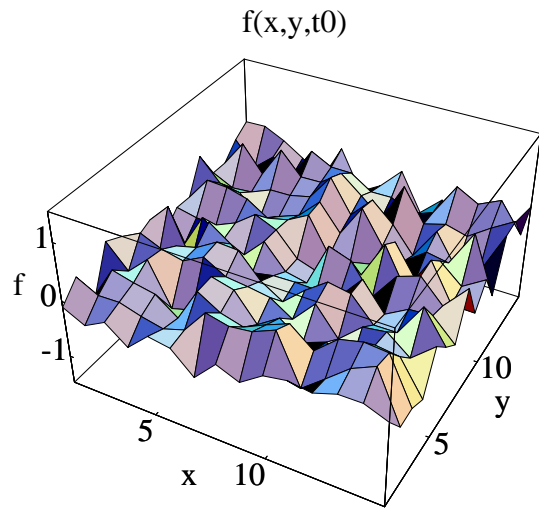
Mean (\pm standard deviation) correlation lengths over the five experiments at various stages of VF. The difference between correlation lengths at 60-61 seconds and those at 3-4 seconds is statistically significant with $p < 0.05$.

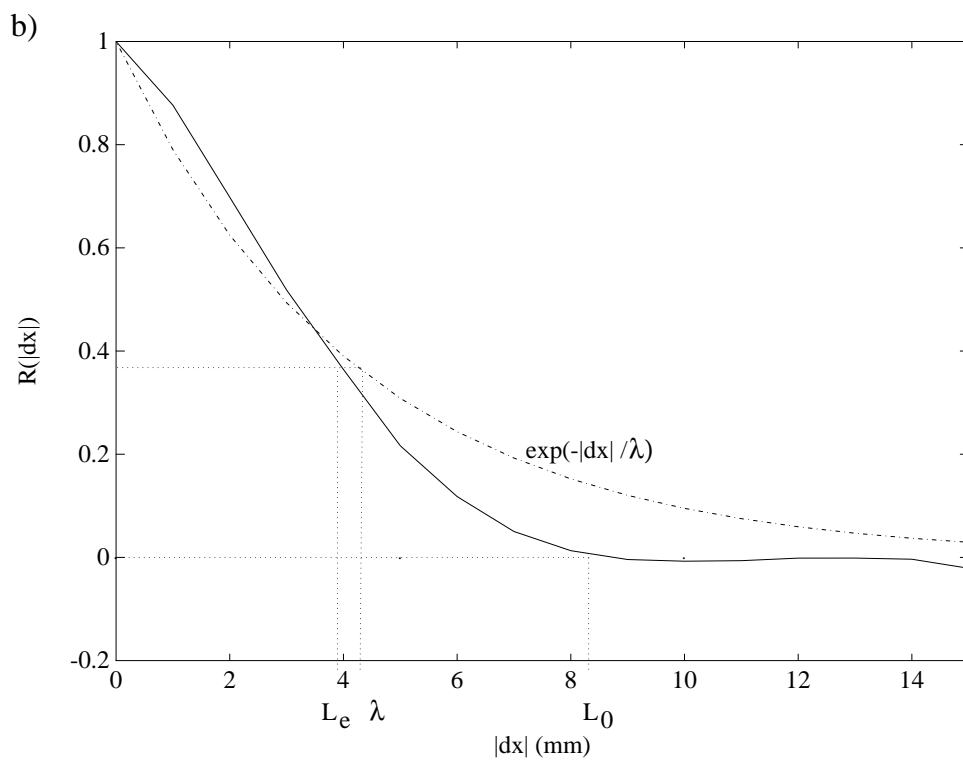
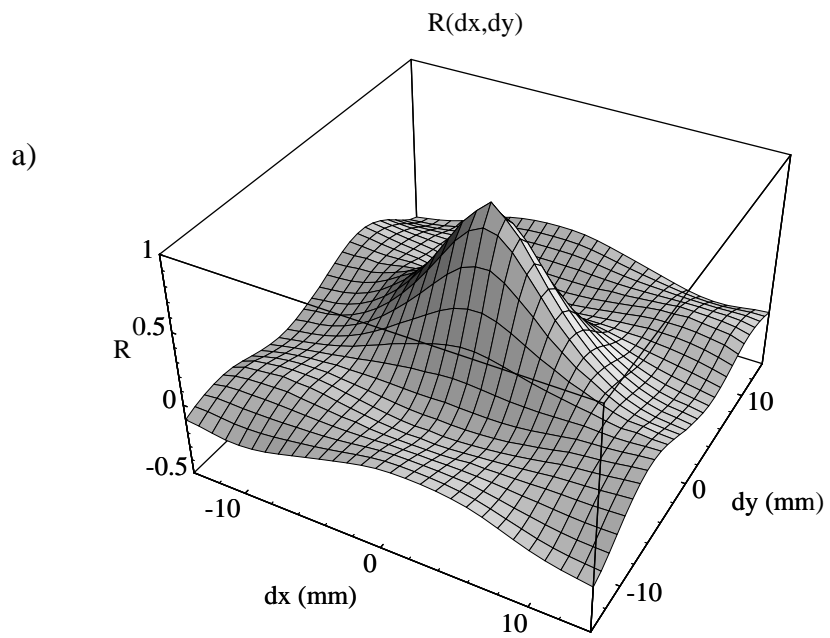
$f(x,y,t_0)$

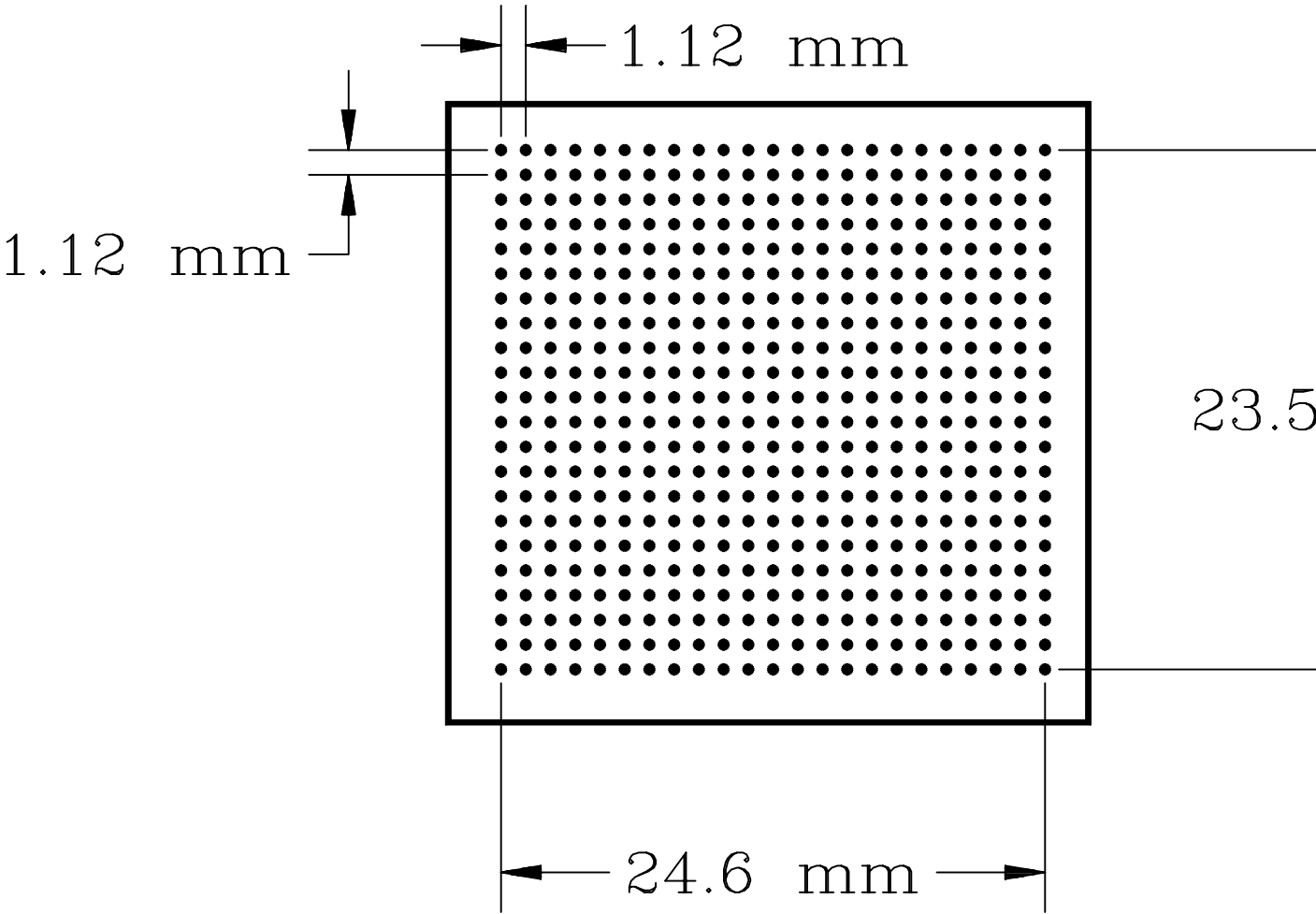


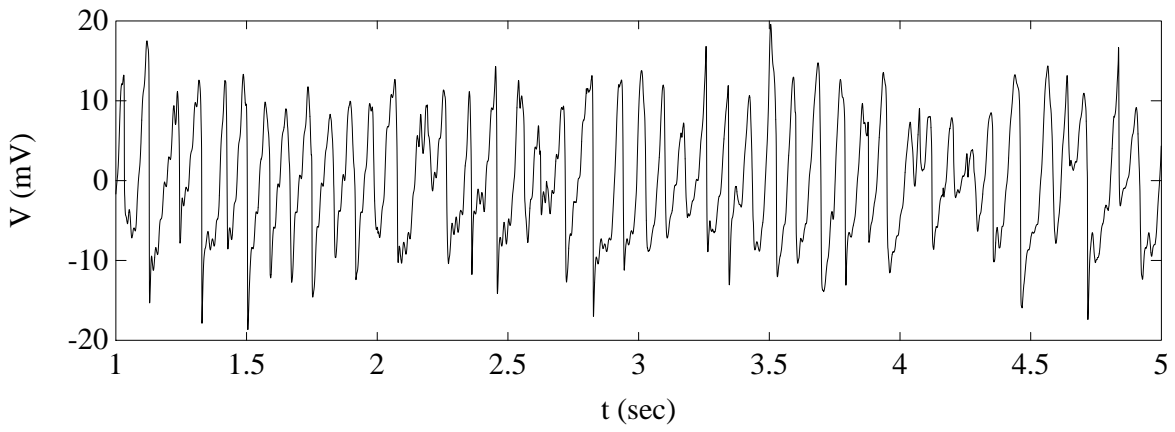
$R(dx,dy)$



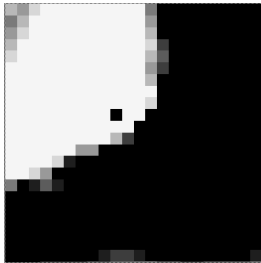




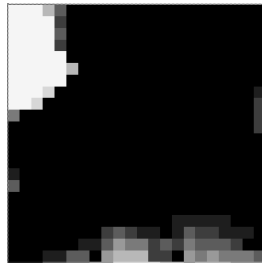




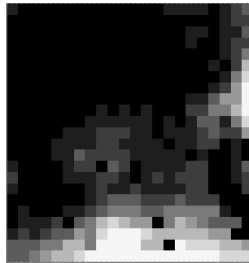
a)



b)



c)



d)



a)



b)



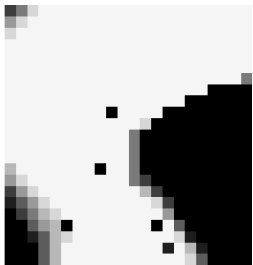
c)



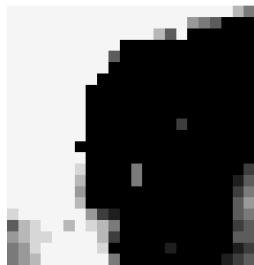
d)



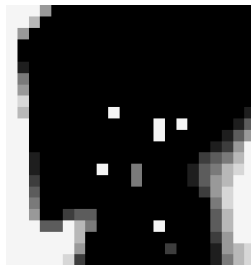
a)



b)



c)



d)



